Vibrational Spectra of Dimethylammonium Paratungstate-B hydrates

Eszter Majzik[1,2], Fernanda Paiva Franguelli[1,2], György Lendvay[1], László Trif[1], Csaba Németh[1], Attila Farkas[3], Szilvia Klébert[1], Imre Miklós Szilágyi[2] and László Kótai[1,4]

[1]*Institute of Materials and Environmental Chemistry, Research Centre for Natural Sciences, ELKH, Magyar Tudósok krt. 2, Budapest, H-1117, Hungary*
[2]*Department of Inorganic and Analytical Chemistry, Budapest University of Technology and Economics, Műegyetem rakpart 3, H-1111, Budapest*
[3]*Department of Organic Chemistry, Budapest University of Technology and Economics, Budapest, Hungary*
[4]*Deuton-X Ltd, Selmeci u. 89, Érd, H-2030, Hungary*

Abstract

Infrared and Raman spectra of two solvatomorphs of a new dimethylammonium polytungstate – decakis(dimethylammonium) dihydrogendodecatungstate – $(Me_2NH_2)(H_2W_{12}O_{42}).nH_2O$ (n=10 or 11) have been evaluated and discussed. The assignation of bands belong to cationic anInfrared and Raman spectra of two solvatomorphs of a new dimethylammonium polytungstate – decakis(dimethylammonium) dihydrogendodecatungstate – $(Me_2NH_2)(H_2W_{12}O_{42}).nH_2O$ (n=10 or 11) have been evaluated and discussed. The assignment of bands corresponding to the cationic and anionic components has been given. The dimethylammonium cation and the crystallization water molecules form a network of regular and multifurcated hydrogen bonds, thus a fraction of the N–H hydrogen atoms are so strongly bound to the anion, that the compound can only be deuterated with an aggressive procedure. The deuterated enneahydrate can be obtained from both solvatomorphs.

Key words: Dimethylammonium dodecatungstate(10-), deuterium isotope exchange, Raman, vibrational spectroscopy

---

1 Introduction

Polytungstates (POTs) represent an extensively studied class of the polyoxometallate family. The structural versatility of these compounds results in an unmatched range of tunable physical properties. [1] [2] [3] [4] Systematic studies on POTs lead to pplications in a wide range of application fields, such as magnetism or catalysis used in medicine or materials science. [5] [6] [7] [8] [9] Dodecatungstates can be isolated as alkylammonium

salts of the equilibrium mixture of hepta - and dodecatungstates containing equilibrium systems. [10] Vibrational spectroscopic studies on polyoxotungstates are limited to a few compounds because the polytungstate cages themselves have a large number of normal modes , and further complications arise when they are combined with alkylammonium cations because then there is massive overlap between the bands characteristic to the units of the compounds – cation, water and anionic cage.

In this work we evaluate the vibrational spectroscopic properties of two decakis(dimethylammonium) dodecatungstate solvatomorphs prepared recently [11] , $(Me_2NH_2)_{10}[H_2W_{12}O_{42}].nH_2O$ with n=10 and n=11) including the IR spectrum of the deuterated enneahydrate, and present the band assignments. We also describe a method for exhaustive deuteration of systems containing inorganic anions and alkylammonium cations that are connected to each other by numerous multifurcated hydrogen bonds.

2 Materials and methods

Chemical grade ammonium paratungstate as WO_3 precursor, 40 % aq. dimethylamine solution, solvents (chloroform, bromoform), deuterium oxide and other analytical reagents were obtained from Deuton-X Ltd., Hungary. $(Me_2NH_2)_{10}[H_2W_{12}O_{42}].10H_2O$ (compound **1)** was prepared from monoclinic WO_3 precursor (prepared by heating of ammonium paratungstate) and 40 % aq. dimethylamine solution according to the procedure given in ref. [11] Recrystallization of compound **1** from water via evaporation to dryness at room temperature resulted in phase pure $(Me_2NH_2)_{10}[H_2W_{12}O_{42}].11H_2O$ (compound **2**). [11]

Deuterated compound **2** was prepared by dissolving of 100 mg of compound in 5 ml of D_2O, then the solution was left to evaporate to dryness when a partially deuterated compound **2** was formed. This partially deuterated **2** was subjected to a four-step exhaustive deuteration procedure, detailed in Section 3.

X-ray powder diffraction measurements were performed at room temperature using a Philips PW-1050 Bragg-Brentano parafocusing goniometer. It was equipped with a copper tube operated at 40 kV and 35 mA tube power, a secondary beam graphite monochromator and a proportional counter. Scans were recorded in step mode. Evaluation of the diffraction patterns had been obtained by full profile fitting techniques.

FT-IR spectra were recorded on a Jasco FT/IR-4600 system. The apparatus was equipped with a Jasco ATR Pro One single reflection diamond ATR accessory (incident angle 45°), and a DLATGS detector used in the 4000-400 cm^{-1} region. A resolution of 4 cm^{-1} and co-addition of 64 individual spectra were applied. An ATR correction (Jasco Spectra Manager version 2/Spectra analysis module version 2.15.11) was performed on the raw spectra. Far-IR spectra were recorded on a BioRad-Digilab FTS-60A far-IR spectrometer with a 6.25 Mylar beam splitter equipped with Pike GladiATR accessory with diamond ATR crystal for the 700-40 cm^{-1} range (nujol mull).

The Raman measurements were performed using a Horiba Jobin-Yvon LabRAM-type microspectrometer with an external 532 nm Nd-YAG (~40mW) or 785 nm diode laser (~50mW) source and an Olympus BX-40 optical microscope. The laser beam was fo-

cused by an objective of 20× (NA=0.4). The confocal hole of 1000 μm and grating monochromators of 1800 and 950 groove mm^{-1} used for excitation wavelengths of 532 and 785 nm, respectively in the confocal system and for light dispersion. In the case of 532 nm excitation the detected wavenumber was scanned with 3 cm^{-1} resolution with data accumulation time 3 s per point (spectral range of 100-4000 cm^{-1}) In the case of 785 nm excitation the spectral range was 100 and 2400 cm^{-1}, 5 cm^{-1} for the resolution and 15 s for the exposure time.

QCC módszerről ide be kell szúrni vmit.

3 Result and Discussion

The reaction of tungsten trioxide and aqueous dimethylamine results dimethylammonium polyoxotungstate compounds, the composition of which strongly depends on the reaction conditions. Thus, under hydrothermal conditions at acidic pH at 150-210 °C a Keggin-type compound ($(Me_2NH_2)_6]H_2W_{12}O_{40}.\sim 4H_2O$) is formed. [12] When the conditions are set differently, we obtain another dodecatungstate. After dissolving WO_3 in an aqueous dimethylamine solution at atmospheric pressure, and slowly eliminating the dimethylamine by evaporation, one decreases the pH until near neutral, when decakis(dimethylamino) paratungstate-B decahydrate, $(Me_2NH_2)_{10}[H_2W_{12}O_{42}].10H_2O$ (compound **1**) is formed. Recrystallization of compound **1** from water turned out not to be feasible, because when it is dissolved in water, instead of **1**, another solvatomorph, the enneahydrate, $(Me_2NH_2)_{10}H_2W_{12}O_{42}.11H_2O$ (compound **2**) crystallizes [11].

In order to facilitate the assignment of IR bands associated with the water and dimethylamine constituents of the crystals of compounds **1** and **2**, deuteration would be helpful. The phenomenon just mentioned prevented us from preparing a deuterated isotopolog of **1** via dissolving it in heavy water: once dissolved, from such solutions only the isotopologs of **2** can be generated. This means that deuteration can provide direct information only about the spectral band of **2**. Deuteration turned out not to be facile. The common method used for replacing H atoms that can dissociate as protons is that one dissolves the compound in heavy water and lets some time for the isotope exchange to take place. This method cannot be expected to provide complete perdeuteration, because the methyl H atoms and the two H atoms inside the dhydrogendodecatungstate cages do not undergo ionic dissociation. However, all water and NH hydrogen atoms should be exchangeable, and the product formed this way will be referred to as 'exhaustively' deuterated compound; in our case it will be denoted as **2-D**. The method, however, proved not to generate exhaustively deuterated dimethylammonium dodecatungstate: only 25% of the NH protons were exchanged this way. [11] For spectrum assignment this is not helpful, so a more aggressive deuteration method was designed.

In every step, 1 hour were allowed for deuterium exchange, after which the HDO formed in the $H_2O+D_2O=2HDO$ and $Me_2NH_2++2D_2O=Me_2ND_2+ + 2HDO$ equilibrium processes was removed by vacuum evaporation using CaO as desiccant. The Ca(OH)(OD) formed was removed after every step and replaced with fresh CaO. The partially deuterated intermediate was dissolved agai nin a new contingent of pure heavy water. The re-

moval of H_2O molecules was considered complete when in the IR spectrum of the product the absorption at the $\delta(H_2O)$ scissor mode in the range of ~1668 and 1616 cm^{-1} disappeared (Fig. 1). At this stage, according to the IR spectrum, the N–H protons are also replaced by D. This aggressive procedure was necessary to ensure that both the dimethylammonium groups and the crystallization water molecules be completely deuterated. The identity of the exhaustively deuterated compound, **2-D** was checked by powder XRD. [11]

The deuteration of compounds **1** and **2** in heavy water produced only the (partially) deuterated form of compound **2**. The reason for this is that compound **1** not only exchanges some of its protons to deuterium but picks up an additional heavy water molecule and crystallizes as compound **2-D**, [11] thus the deuterated form of compound **1** cannot be prepared. Thermal dehydration of compound **2** does not give compound **1**, because several water molecules are lost in its first thermal decomposition step. [13] To achieve exhaustive deuterium exchange (of all N–H and O–H protons except those two that are in the cage's internal O–H groups), the four-step exhaustive deuteration procedure described in the methods section was performed. In more details, high excess of deuterium oxide was applied in the first step (by setting 50-fold D/H ratio), and the same amount of D_2O was used in every additional step, but the D/H ratio was increased to the ratio of D/H achieved in the products of the previous cycle. Thus, starting from either **1** or **2**, after crystallization we obtained the completely (42-fold) deuterated form of compound **2 (2-D)**.

3.1 General vibrational spectroscopic features of compounds 1, 2 and 2-D

The IR spectra of compounds **1** and **2** and the exhaustively deuterated **2-D** are shown in Fig. 1. The positions of the band maxima and their assignments are given in Table 1 and ESI Figs. 1-3. Overall, the IR spectra of compounds **1** and **2** are very similar. This shows that the main structural motifs are identical in both compounds. The observed bands corresponding to the crystallization water, the dodecatungstate cage and the dimethylammonium cations strongly overlap in the spectra of both **1** and **2**. To identify of spectral bands corresponding to each group, deuteration had to be used which can help to resolve the congested spectra.

The vibrational frequencies of water molecules could, in principle, be identified by finding the bands that disappear upon dehydration. However, stoichiometrically pure thermal dehydration of the crystals of compounds **1** and **2** is not feasible because they chemically transform during thermal treatment with loss of water and dimethylamine molecules simultaneously. [13] Exhaustive deuteration allowed us to separate the bands corresponding to the deuterium exchangeable O–H and N–H bonds in the water of crystallization molecules and dimethylammonium ions from those of the non-exchangeable hydrogen-containing groups (dihydrogendodecatungstate cage, methyl groups) or groups without hydrogens (e.g. modes of C-N bonds).

Raman spectroscopy is a useful method to clarify the nature of polytungstate cages, [14],thus, the Raman spectrum of compound **1** was also studied in detail to

TABLE 1
IR spectroscopic modes and their assignations for compounds **1, 2** and **2-D**

Assigment	**IR wavenumber, cm $^{-1}$**		
	1	**2**	**2-D**
$\nu_s(OH)$ and $\nu_{as}(OH)$	3317 br	3317 br	2496, br
$\nu(OH)$ internal	(combined band system)	(combined band system)	3373 (non-deuterated)
$\nu_{as}(CH)$	3032 (br)	3030	3026
$\nu_s(NH)$ and $\nu_{as}(NH)$	3012	3013 br	2276, 2213
$\nu_{as}(CH)$	2961	2961.0	2964, 2960
$2 \times \omega(NH_2)$	2858	2860	2112 br
$2 \times \delta_s(CH_3)$	2777	2778	2780-2760, br
$\nu(NH)$ (ν_3)	2746sh	2755 sh	2125-2047, br
$\omega(NH_2)(B_1) + \nu(CN)(B1)$	2439	2442	1864, br and 2085 br
$\rho(NH_2)(B1) + \delta(NH_2)(B_1)$			
$\delta(OH)$	1668, 1624, 1615	1668, 1623,1616	1228, 1208
$\delta(NH_2)$	1580, 1569	1581 (m)	1161
$\delta_{as}(CH)$	1460, 1431, 1414	1459, 1439sh, 1415	1456, 1433,1415
$\omega(NH_2)$	~1430, covered	~1430, covered	1151
$\delta_s(CH_3)$	1402	1402.0	1408
$\rho_s(CH_3)$	1227	1231	1228
$2 \times \rho(H_2O)$	1090	1089	861sh
$\nu(CN)$	1018	1023, 1016	1024
$\nu(W=O)_{term}$, $\delta(OH)_{int}$	954	954.5,	955sh
$\nu(WO_2)_{term}$	943	943, 933	931
$\nu(W-O-W)_{edge}$ (stretching and bending modes)	887sh	888	888
$\rho(NH_2)$	898sh	873	683
$\nu(CN)$			
$\nu(W-O-W)_{edge}$ (bending and stretching) modes	850	850	848sh
$\nu(W-O-W)_{edge}$ (stretching and bending modes)	826	819, 808	811, 807sh
$\nu(W-O-W)_{corner}$ (stretching and bending modes)	746, 719, 638, 605	777, 726, 665, 610	743, 715sh, 652, 613
$\rho(OH)_{int}$	550	549	549sh, 532
$\delta(WO_2)$	476	490	484, 434
$\delta(NC_2)$	417sh	433	410
$\delta(OH)_{int}$ and $\delta(WO_2)$	402	399	401
$\delta(WO_2)$	360, 345,307	374 336, 310	355, 336, 310
Lattice modes	152, 127sh, 97, 80	276,. 240, 139, 101, 80, 62	271, 240, 143, 99, 83, 61

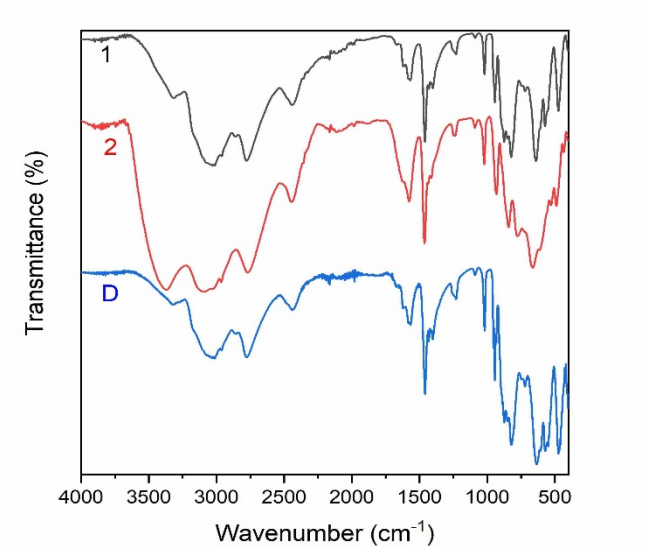

FIGURE 1: IR spectra of compounds **1** (black), **2** (red) and **2-D** (blue).

distinguish the bands corresponding to the polyanion from those characterizing the other constituents of the compound (Table 2, ESI Fig. 4).

TABLE 2
Raman shifts in $cm^{-1}$for the $H_2W_{12}O_{42}$(10-) cage of compound **1** at 532 and 785 nm laser excitation at room temperature

Assignation	**Raman bands**	
	532 nm	**785 nm**
$\nu(W=O)_{term}$	956, 942, 934	955, 936sh
$\nu(W-O-W)_{edge}$	911,899,883,873,857	908,891,886,874, 857
$\nu(W-O-W)_{corner}$	722 br, vw	724 br, vw
$\nu(W-O-W)_{edge,corner}$	580, 562	644, 580, 557br, 497
$\delta(WO_2)$	403,356	405, 359, 350sh

Vibrational modes of crystallization water

Water molecules with C_{2v} symmetry have three normal modes, and all three vibrations are both infrared- and Raman-active. The wide $\nu(OH)$ band system centered around 3317 cm^{-1}in the spectra of compounds **1** and **2**consists of the $\nu(OH)$bands of water and $\nu(OH)$ modes of internal OH groups in the polytungstate cage. Since the latter are strongly bound inside the cage with three oxygen they are not involved in deuterium exchange [15] [16] [17], Accordingly, from the wide band by deuteration only the contribution of water of crystallization can be eliminated, and the component corresponding to the OH stretch ($\nu(OH)_{int}$) of the internal OH bond does not change. As a result, when **2** was deuterated, in the IR spectrum of **2-D** the intensity of the originally combined peak was found to decrease ,while its center was shifted to 3373 cm^{-1}. This means that the latter band can be assigned to the intra-cage OH group of the dihydrogendodecatungstate ion. The component of the IR band corresponding to the crystallization water stretching

vibration is centered at a lower wavelength than 3373 cm^{-1}, but its exact position cannot be revealed.

The scissor mode of water molecules appears as a complex band system in the IR spectra of compounds **1** and **2**, at 1668, 1624 or 1615 and 1668, 1623 or 1616 cm^{-1}, respectively. This shows that the H_2O molecules are located in at least three different environments. This assignment is confirmed by the observation that upon deuteration of compound **2**, this complex band system disappeared and two unresolved band systems appeared at 1228 and 1208 cm^{-1}.

3.2 Characterization of the vibrational modes of the dodecatungstate anion

The condensed WO_6 octahedra build the same type of $H_2W_{12}O_{42}{}^{10-}$ cage in both **1** and **2** [11]. The bare polyoxometallate cage in the crystal has 168 normal modes [18], and the IR-active ones can be expected to appear in the spectra of both compounds. Here we focus on the vibrations of the W–O framework, the frequencies of which are below 1000 cm^{-1} (and, as expected, are all insensitive to deuteration). There are numerous similar bonds in the cages, which strongly interact. We performed density functional (DFT) calculations at the CAM-B3LYP/LANL2DZ level on several model systems ($H_2W_{12}O_{42}{}^{10-}$ cage fully protonated or four-fold protonated and six-fold coordinated by dimethylammonium or 10-fold coordinated by dimethylammonium). In all cases, the corresponding intra-cage modes proved to be very similar. All of them are non-local, *i.e.*, the vibration associated with them involves many W and O atoms in extended ranges of the cluster. No single stretching or bending modes can be distinguished; instead, there are some modes consisting of combinations mostly one kind of e.g. W–O stretching motion in different parts of the cage, and many are combinations involving several kinds of motions (e.g. both W–O and W=O stretching, often even bending), as it is known from the experimental literature, too. [19] The calculated frequencies are not directly comparable with the experimental ones, so in the following the calculated results will be associated with the experimental ones according the relative magnitude of the frequencies. In the IR spectroscopy of tungstate cages, the known W–O stretching modes include those corresponding to two different types of terminal W=O and $W(=O)_2$ groups (1000-960 cm^{-1}), those associated with two types of bridging W-O-W groups (octahedral edge sharing at 800-760 cm^{-1} and corner sharing at 890-850 cm^{-1}). [18]

In the IR spectra of both compounds **1** and **2**, most of the characteristic frequencies associated with the cage vibrations appear between about 940 and 1000 cm^{-1} and between 400 and 500 cm^{-1}. The terminal W=O modes can be assigned to the peaks at 957 and 955 cm^{-1}, respectively. According to the DFT calculations, the highest-frequency cluster modes are combinations of mostly terminal W=O stretches. The latter band probably contains the $\delta(\mathrm{OH})$ mode of the internal OH groups appears exactly at the same frequency for both compounds **1** and **2**. [20] The positions of these bands cannot be changed by deuteration, because, as explained above, the H atoms of the internal OH groups in polytungstates are not deuterium exchangeable. [15] [16] [17]

The $\nu(\mathrm{W}(=\mathrm{O})_2)$ and the $\delta(\mathrm{W}(=\mathrm{O})_2)$ modes can be assigned at 942 and 943/933

cm^{-1} as well as at 471 and 474/458 cm^{-1} in the IR spectra of the compounds **1** and **2**, respectively. [18]

There are three intense Raman bands in the spectrum of compound **1** that can be assigned to W=O and W(=O)$_2$ type terminal units, at 967, 950 and 930 cm^{-1}if the excitation is at 532 nm and at 955 and 936 cm^{-1} when the excitation wavelength is 785 nm. The most intense Raman band is that at around 950 cm^{-1}. The location of these bands is exactly the same as those of the $\nu(\mathrm{W=O})_{\mathrm{term}}$ and $\nu(\mathrm{W(=O)_2})_{\mathrm{term}}$ bands observed at 967 and 950/930 cm^{-1} in the Raman spectrum of sodium dodecatungstate(10-). [18] The deformation modes of (W(=O)$_2$)$_t$ groups are located between 400 and 300 cm^{-1}. The deconvolution of the complex band shown in Fig. **2** resulted in three maxima at 339, 367 and 396 cm-1. The Raman band located at 396 cm^{-1} is close to the non-deuterable $\nu(OH)_{\mathrm{int}}$IR mode found around 400 $cm^{-1}$to assign this while the other two bands are assigned as terminal W(=O)$_2$ modes. The strong IR bands of compounds **1** and **2** and the weak/moderately intense Raman peaks of compound **1** between 920 and 500 cm^{-1} belong to the edge (>800 cm^{-1}) and corner-shared (800-700 cm^{-1}) W-O-W modes, [18] respectively (Tables 1 and 2). Some mixed corner- and edge-shared modes can also be identified between 650 and 475 cm^{-1} in the Raman spectrum. The $\rho(\mathrm{OH})$ libration mode of the internal OH group is expected to appear between 600 and 500 cm^{-1},[17] where the bands of mixed modes also located. Accordingly, the Raman spectrum of compound **1** is complicated in this range. Deconvolution of the bands resulted in four components. The lowest-frequency band centered at 549 corresponds to the $\rho(\mathrm{OH})_{\mathrm{int}}$ libration), [20] while the other three bands that probably belong to the mixed $\nu(\mathrm{W-O-W})$ modes are centered at 573, 600 and 644 cm^{-1} (Fig. 2).

The lattice modes are all located below 300 cm^{-1}as it can be seen in the far-IR spectra of compounds **1, 2, 2-D** (ESI Fig. 1-3, respectively) and also in the Raman spectrum of compound **1** (ESI Fig. 4). This part of the spectrum is poorly resolved and cannot be assigned to any particular kind of vibration.

The vibrational modes of the intra-cage OH groups also appear in the spectra of **1** and **2**. Arnaiz et al. et al. [20] assigned a mixed IR band to the internal OH group and the crystallization water of 2-ethylpyridinium dodecatungstate monohydrate at ~3420 cm^{-1}, and two other bands were assigned to the internal OH groups at 965 and 410 cm^{-1}. These modes were found in the IR spectra of both **1** and **2**, at wavenumbers 3317(3373), 955 and 402 as well as 3317(3373), 955 and 399 cm^{-1}, respectively (Table 1). The band at ~399 cm^{-1} in the IR spectrum of **2** remain at the same location after deuteration (intra-cage OH group).

3.3 Vibrational modes of dimethylammonium cations

The free dimethylammonium cation, ($Me_2NH_2^+$, overall symmetry is C_{2v}) has 27 internal modes distributed as $9A_1$+$5A_2$+$7B_1$+$6B_2$ and are represented as $\nu_1 - \nu_{27}$ in ESI Table 1. [21] [22] The A_2 modes are only Raman active, while the rest of the modes are both IR and Raman active. The presence of strong hydrogen bonds results in reduction of the $\nu(\mathrm{NH})$ stretching frequencies shifting the $\nu(\mathrm{NH})$ bands into overlap with the $\nu(\mathrm{CH})$ bands around ~ 3000 cm^{-1}. The stretching bands of the cations in compound **2** were

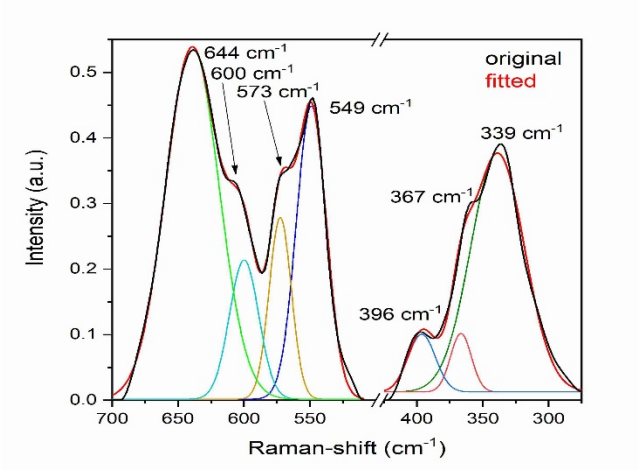

FIGURE 2: Deconvolution of Raman bands for**1** in the frequency range of $(W{=}O_2)_t$, $(O\text{-}W\text{-}O)_{e,c}$ and (O-H) modes

separated using deuteration. The bands at ~3030 and 2961 cm^{-1} remained unchanged and are assigned to correspond to the $\nu_{as}(CH)$ and $\nu_s(CH)$modes. The bands located at ~3013 and 2755 cm^{-1} were shifted to 2276-2213 and 2125-2047 cm^{-1}. The ratio of the frequencies seen in the protiated and the deuterated isotopolog is 1.34 or 1.32, respectively (Table 1), close to the ν_{NH} /ν_{ND} = ~1.35 ratio typical to stretch mode shifts. [23]The overtone of the $\delta(CH_3)$ deformation band ($2 \times \delta(CH_3)$ is expected to appear at around 2780 cm^{-1}. Thus, the peak observed at 2778 cm^{-1} in the spectrum of **2**, and remained unchanged upon deuteration, is assigned to this mode.

The bending modes of the NH_2^+ group expected to appear near 1600cm^{-1} (scissor mode), at about 880 cm^{-1} rocking mode) and 1430 cm^{-1} (ω mode of NH_2) In the spectrum of compound **2** are one can identify a peak at ~1581), at ~873 and a broad system at ~1430 cm^{-1}. The first two and a part of the third are shifted to 1161, 683 and 1151 cm^{-1} upon deuteration. The ν_{NH} /ν_{ND} ratios are 1.36, 1.28 and 1.24, close to the expected values, so these peaks are assigned to the NH_2 scissor, rocking and ω modes, respectively.

The IR band observable at 2440 cm-1 in the spectrum of **1** and at 2442 cm^{-1} in that of **2**may correspond tothe combination of the wagging (B_1) mode of the $Me_2NH_2^+$ group with its $\nu(CN)(B1)$mode or to the combination of the $\rho(NH_2)$ (B1) and $\delta(NH_2)$ (B1) modes of B_1 symmetry. The deuteration shifted the band into two broad band systems centered at 1864 and 2085 cm^{-1}, which may be attributed to the combinations of $\rho(ND_2)$ (B_1) + $\nu(CN)$ (B_1) and $\rho(ND_2)$ (B_1) + $\delta(ND_2)$ (B_1) modes, respectively (Table 1). This indicates that the bands found near 2440 cm^{-1} in fact consist of two distinct but overlapping combination bands.

The expected position of the band corresponding to the $\omega(NH_2)$ mode (~1430 cm^{-1} for both compounds **1** and **2**) can overlap with one of the $\delta_{as}(CH_3)$ bands (Table 1). On deuteration, the shape of the band system around 1430 cm^{-1} changed due to the removal of the $\omega(NH_2)$component. The component whose position has not changed can

be assigned to the $\delta_{\mathrm{as}}(\mathrm{CH_3})$ mode. There is a signal of the $\omega(\mathrm{ND_2})$ band a 1051 $\mathrm{cm^{-1}}$ and its overtone at around 2100 $\mathrm{cm^{-1}}$ in the spectrum of deuterated **2-D** which are missing from those of the undeuterated compounds. The analogous overtone peaks of the $\omega(\mathrm{NH_2})$ mode can be expected and seen at 2860 $\mathrm{cm^{-1}}$ in the non-deuterated compound **2**; thus, the broad band system observed in the IR spectra of the non-deuterated compounds **1** and **2** contains the contribution from the $\omega(\mathrm{NH_2})$ mode associated with the broad band system centered around 1430 $\mathrm{cm^{-1}}$ (Table 1).

The Raman spectra recorded at 532 nm excitation frequency display some bands characteristic for of C–H and N-H modes around ~2800, ~2850, ~2970 and ~3060 $\mathrm{cm^{-1}}$. These bands are wide and consist of different bands of each type of cations (ESI Fig. 4).

4 Conclusion

Vibrational spectra (IR, Raman and far-IR) of two solvatomorphs of dimethylammonium polytungstate – decakis(dimethyl-ammonium) dodecatungstate – $((\mathrm{Me_2NH_2})_{10}\mathrm{W_{12}O_{42}}).n\mathrm{H_2O}$(n=10 or 11) **1** and **2** have been recorded and evaluated in detail. To collect additional data the compounds were deuterated. Due to the multifurcated hydrogenbond systems existing in these hydrates, the deuteration can be done only with an agressive deuteration procedure involving repeated dissolution–solvent evaporation steps, which yielded the exhaustively deuterated enneahydrate (in which all exchangeable H atoms are substituted by D, and the $\mathrm{CH_3}$ and intracage H atoms remain protiums). The same product was obtained from both solvatomorphs, because after dissolution of either of them in water, the enneahydrate crystallizes. The comparison of the IR spectra of deuterated (**2-D**) and undeuterated enneahydate crystals allowed us to separate the contributions of different structural units to congested band system different part of compound **2** was performed with comparing the IR bands of deuterated and non-deuterated compound **2**. The IR, Raman and far-IR spectra spectra of compound **1** were also evaluated to distinguish the bands belong to each mode of polytungstate cage. The vibrational spectroscopic character of polytungstate cage were found to be the same in both solvatomorphs.

ACKNOWLEDGMENTS

The research within project No. VEKOP-2.3.2-16-2017-00013 and GINOP-2.2.1-15-2017-00084 was supported by the European Union and the State of Hungary, co-financed by the European Regional Development Fund.

References

[1] Xie, F., Li, X., Li, Y.J., Jiang, X.S., Rui, Q., and Sha, J.Q. (2019) Assembly of polyoxometalate-templated metal-organic framework with effective peroxidase-like catalytic activity. *J. Coord. Chem*, **72** (2), 272–282. URL https://doi.org/10.1080/00958972.2018.1554215.

[2] Shakeela, K. and Rao, G.R. (2018) Thermoreversible, Hydrophobic Ionic Liquids of Keggin-type Polyanions and Their Application for the Removal of Metal Ions from Water. *ACS Applied Nano Materials*, **1** (9), 4642–4651, doi:10.1021/acsanm.8b00920. URL https://dx.doi.org/10.1021/acsanm.8b00920.

[3] Khan, S.U., Akhtar, M., Khan, F.U., Peng, J., Hussain, A., Shi, H., Du, J., Yan, G., and Li, Y. (2018) Polyoxometalates decorated with metal-organic moieties as new molecular photo- and electro-catalysts. *Journal of Coordination Chemistry*, **71** (16-18), 2604–2621, doi:10.1080/00958972.2018.1500694. URL https://dx.doi.org/10.1080/00958972.2018.1500694.

[4] Chen, S.A. and Xu, X.X. (2018) The loading of polyoxometalates compound on a biomass derived N-doped mesoporous carbon matrix, a composite material for electrolytical energy storage. *Journal of Coordination Chemistry*, **71**, 3035–3044. URL https://doi.org/10.1080/00958972.2018.1508661.

[5] Neelam, D.M., Burg, A., Shamir, D., and Albo, Y. (2018) Polyoxometalates entrapped in sol-gel matrices as electron exchange columns and catalysts for the reductive de-halogenation of halo-organic acids in water. *Journal of Coordination Chemistry*, **71** (19), 3180–3193, doi:10.1080/00958972.2018.1515926. URL https://dx.doi.org/10.1080/00958972.2018.1515926.

[6] Li, X., Wang, Y.L., Zhou, K.F., Wang, Y.L., Han, T., and Sha, J.Q. (2018) Isomeric organic ligand dominating polyoxometalate-based hybrid compounds: synthesis and as electrocatalysts and pH-sensitive probes. *J. Coord. Chem*, **71** (3), 468–482. URL https://doi.org/10.1080/00958972.2018.1443216.

[7] Jumabekov, A.N., Lloyd, J.A., Bacal, D.M., Bach, U., and Chesman, A.S.R. (2018) Fabrication of Back-Contact Electrodes Using Modified Natural Lithography. *ACS Applied Energy Materials*, **1** (3), 1077–1082, doi:10.1021/acsaem.7b00213. URL https://dx.doi.org/10.1021/acsaem.7b00213.

[8] Yamase, T. (2019) Isopoly and Heteropoly Compounds of Molybdenum, Tungsten, and Vanadium. *Eur. J. Inorg. Chem*, (3-4), 343–345. URL https://doi.org/10.1002/ejic.201801308.

[9] Olenin, A., Yu, Mingalev, P.G., and Lisichkin, G.V. (2018) Advancement in Catalysts for Transesterification in the Production of Biodiesel: A Review. *Petroleum. Chem*, **58** (8), 577–592. URL https://doi.org/10.1134/S0965544118080182.

[10] Cruywagen, J.J. (2000) Protonation, oligomerization, and condensation reactions of vanadate(V), molybdate(VI) and tungstate(VI). *Adv. Inorg. Chem*, **49**, 127–182. URL https://doi.org/10.1016/S0898-8838(08)60270-6.

[11] Lendvay, G., Majzik, E., Bereczki, L., Domján, A., Trif, L., Sajó, I.E., Franguelli, F.P., Farkas, A., Klébert, S., Bombicz, P., Németh, C., Szilágyi, I.M., and Kótai, L. (2020) Dodecatungstate cages embedded in a variable dimethylammonium

cation+water of crystallization matrix in the new. *J. Am. Chem. Soc*, (Me2NH2), 10–10.

[12] Zavalij, P., Guo, J., Whittingham, M.S., Jacobson, R.A., Pecharsky, V., Bucher, C.K., and Hwu, S.J. (1996) Keggin Cluster Formation by Hydrothermal Reaction of Tungsten Trioxide with Methyl Substituted Ammonium: The Crystal Structure of Two Novel Compounds, [NH2(CH3)2]6H2W12O40· ∼4H2O and [N(CH3)4]6H2W12O40· 2H2O. *Journal of Solid State Chemistry*, **123** (1), 83–92, doi:10.1006/jssc.1996.0155. URL https://dx.doi.org/10.1006/jssc.1996.0155.

[13] Trif, L., Lendvay, G., Franguelli, F.P., Majzik, Bereczki, L., Szilágyi, I.M., and Kótai, L. (2020) Thermal analysis of solvatomorphic decakis(dimethylammoni-um) dihydrododecatungstate hydrates. *Journal of Thermal Analy-sis and Calorimetry*.

[14] Liu, S., Chen, Q., Zhang, P., and Li, S. (1998) Raman spectral study on isopolytungstates in aqueous solutions. *Trans. Nonferrous Metal Soc*, **8** (4), 688–692.

[15] Fait, M., Heidemann, D., and Lunk, H.J. (1999) Characterization of the protons in polycrystalline paratungstates using 1H MAS NMR investigations. *Z. Anorg. Allgem. Chem*, **625** (3), 530–538. URL https://doi.org/10.1002/(SICI)1521-3749(199903)625:3<530::AID-ZAAC530>3.0.CO;2-K.

[16] Evans, H.T. and Prince, E. (1983) Location of internal hydrogen atoms in the paradodecatungstate polyanion by neutron diffraction. *Journal of the American Chemical Society*, **105** (14), 4838–4839, doi:10.1021/ja00352a054. URL https://dx.doi.org/10.1021/ja00352a054.

[17] Launay, J.P., Boyer, M., and Chauveau, F. (1976) High resolution PMR of several isopolytungstates and related compounds. *Journal of Inorganic and Nuclear Chemistry*, **38** (2), 243–247, doi:10.1016/0022-1902(76)80402-2. URL https://dx.doi.org/10.1016/0022-1902(76)80402-2.

[18] George, B.L., Aruldhas, G., and Botto, I.L. (1992) Vibrational spectra of sodium paratungstate 26 hydrate, Na10(H2W12O42)26H2O. *Journal of Materials Science Letters*, **11** (21), 1421–1423, doi:10.1007/bf00729648. URL https://dx.doi.org/10.1007/bf00729648.

[19] Rocchiccioli-Deltcheff, C., Fournier, M., Franck, R., and Thouvenot, R. (1983) Vibrational investigations of polyoxometalates. 2. Evidence for anion-anion interactions in molybdenum(VI) and tungsten(VI) compounds related to the Keggin structure. *Inorganic Chemistry*, **22** (2), 207–216, doi:10.1021/ic00144a006. URL https://dx.doi.org/10.1021/ic00144a006.

[20] Arnaiz, A., Cuadrado, L., Santiago, C., Lorente, L., and Arrieta, J.M. (1987) Synthesis, characterization and thermogravimetric decomposition of 2-ethylpyridinium metatungstate monohydrate. Kinetic study of its thermal dehydration. *Journal of Thermal Analysis*, **32** (5), 1449–1456, doi:10.1007/bf01913345. URL https://dx.doi.org/10.1007/bf01913345.

[21] Bellanato, J. (1960) Infra-red spectra of ethylenediamine dihydrochloride and other amine hydrochlorides in alkali halide disks. *Spectrochim. Acta*, **16**, 80 008–80 010. URL https://doi.org/10.1016/S0371-1951(60)80008-2.

[22] Ebsworth, E.A.V. and Sheppard, N. (1959) The infra-red spectra of some methylammonium iodides: angle deformation frequencies of and 2 groups. *Spectrochimica Acta*, **13** (4), 261–270, doi:10.1016/0371-1951(59)80026-6. URL https://dx.doi.org/10.1016/0371-1951(59)80026-6.

[23] Krimm, S. (1960) Approximate isotopic frequency rule and is application to the spectra of complex molecules. *J. Chem. Phys*, **32** (6), 1780–1783. URL https://doi.org/10.1063/1.1731020.